

Variation in fecundity and condition of yellowtail flounder, *Limanda ferruginea*: patterns across stocks over ten years

Mark Wuenschel, Dave McElroy, Richard McBride-

NEFSC

Emilee Tholke, Yvonna Press-

CONTRACTORS FOR IBSS IN SUPPORT OF NOAA FISHERIES

### Background/rationale

Sustainable management of fisheries requires maintaining the reproductive capacity of a stock. Spawning stock biomass often used as a proxy for total egg production, assumes egg production is a constant function of size or weight. Increasingly, as fecundity data becomes more readily available, many of these assumptions are being challenged. Specifically, studies have shown that larger and/or older females produce proportionally more and better eggs (Berkeley et al. 2004, Hixon et al., 2014, Jeuthe et al. 2013, Barneche et al. 2018). In addition, for the rare cases where time-series of fecundity is available, annual variation has been documented and linked to environmental drivers acting during oocyte development (dos Santos Schmidt et al. 2017, 2020). Despite the importance of understanding the factors regulating fecundity variation, fecundity remains one of the most poorly measured life history parameters of marine fishes (Tomkiewicz et al. 2003). However, recent advances via semi-automated processing (Thorsen and Kjesbu 2001) has enabled the routine collection of fecundity data, including those reported here.

Yellowtail flounder life history with respect to reproduction and energetics have been studied in the region (McElroy et al., 2015; Wuenschel et al. 2019). By evaluating the longer time series of data now available, we may be able to better understand the allometry of fecundity and the linkages between environmental drivers of fecundity. For example, yellowtail flounder appear to set an optimistic upper limit for fecundity during early oocyte development, but undergo levels of down-regulation of fecundity to better match their energetic status.

In collaboration with NEFSC CRP's Study Fleet, yellowtail flounder (three stocks) have been sampled since 2010 to supplement samples collected on NEFSC annual Spring Bottom trawl surveys to determine fecundity. Analysis of the first few years of data indicated significant positive allometry in PAF as a function of length and significant year and stock effects on potential annual fecundity (McElroy et al. 2015), suggesting environmental regulation at regional scale. McElroy et al. (2015) also reported annual variation in relative condition, which was related to the amount oocyte atresia in females. These earlier studies generated the following working hypotheses from a general bioenergetics framework. First, the fecundity-size relationship is hyper-allometric, i.e. as size increases, fecundity increases at a greater proportion

than weight does. This indicates that a given biomass of larger females produce more eggs than an equal biomass of smaller females. This maternal effect is not usually considered in assessments of population reproductive potential. Secondly, reproductive investment of fishes derives from surplus energy (McBride et al. 2015), and as such may be regulated by and related to various physiological drivers (e.g. body or liver condition). Therefore annual variation in environmental productivity that effects fish condition results in variable energy available to reproduction, which manifests as annual variation in fecundity.

Following on these working hypotheses, our specific goals were to explore the allometry of the size-fecundity relation to determine if significant maternal effects (in terms of egg numbers) exist for yellowtail flounder, and the potential implications of such patterns with subsequent concurrent changes in stock demographics. Acknowledging that physiological aspects of fish condition regulate potential fecundity, we determined the importance of size, relative condition (weight at length), and hepato-somatic index explain variation in fecundity across time (years) and space (stocks). Given the ease of collecting relative condition data as compared to fecundity estimates, we also explore the relation between the two and potential limitations of using existing long-term time series.

## Methods

The data presented here represents a continuation of the McElroy et al. (2015) study, which provides a more detailed explanation of the sampling methods, and specific protocols for fecundity determination of yellowtail flounder. In short, we continued sampling and processing in the same manner and now report on ten years of data (Table 1). Samples were collected over the three stocks, covering a broad geographical range (Figure 1). The majority of samples (~82%) came from the NEFSC CRP Study fleet, with remainder (~18%) coming from fishery independent surveys (NEFSC and MADMF).

Relative condition ( $K_n$ ; observed weight/ predicted weight) was calculated following Wuenschel et al. (2019), using the length weight equation they developed from samples throughout the year to predict weight from length.

Liver condition was assessed by calculating the hepatosomatic index (HSI;  $100 \times (\text{liver weight} / (\text{total weight} - \text{liver weight}))$ ). Liver weights were not available for all samples.

The allometry of the fecundity vs. weight relation was tested by fitting the following to the full dataset (i.e. all fish, across all stocks including fish without liver weights):

$\text{Log (Fecundity)} \sim \text{Log (Weight)}$

to obtain the intercept and slope. Since we wished to test if the slope was significantly different than 1, we used an offset of one to test for the significance of the slope term to obtain a p value.

To explore the variation in fecundity, we modeled for the following GLM in R:

$\text{Log(Fecundity)} \sim \text{Log(TL)} + K_n + \text{HSI} + \text{MEANOD} + \text{Stock} + \text{Year} + \text{Stock:Year}$

where TL, Kn, HSI are as described above, and MEANOD is the mean oocyte diameter of the developing clutch of oocytes to be spawned, which indicates the nearness (developmentally) to spawning. Stock, Year, and Stock:Year terms were included to account for potential spatial and temporal variation in fecundity that may or may not be synchronized across stocks. A stepwise selection process was used to select the combination of terms making the best overall model with the lowest AIC score.

We compared patterns in relative condition of the ‘fecundity fish’ to the available time series of relative condition of developing females from spring bottom trawl survey to explore the utility of the time series as a proxy for fecundity. First, for the available NEFSC spring bottom trawl survey time series where individual weights are available (1992-2023) we calculated Kn as described above for each stock using the strata listed in Table 4. Second, for the fecundity fish, that have additional physiological metrics, we were able to model Kn as a function of length, HSI, MEANOD, Stock, Year and Stock:Year. This allowed us to obtain a more detailed estimate of Kn for these ‘fecundity fish’ that accounts for the other significant variables affecting fecundity. The two time series were plotted alongside each other to visually assess the similarity in patterns of annual estimates.

## Results and Discussion

The large amount of fecundity data collected over 10 years allowed us to determine the scaling relationship between annual fecundity and weight. An earlier analysis on the first three years of the fecundity data presented (McElroy et al. 2015), indicated the slope of the fecundity relation with fish length was significantly greater than 3 (for GOM and SNE stocks), but did not specifically test whether it was greater than the length-weight exponent, or if the fecundity-weight exponent was greater than 1. The present analysis provides definitive evidence that the fecundity of yellowtail flounder increases hyperallometrically with weight (i.e. the fecundity allometry vs size is greater than the weight allometry vs length). Fish weight alone explained a large amount of variation in fecundity ( $r^2 = 0.71$ ), and the exponent of 1.33 was significantly greater than one (Table 2, Figure 2). This hyperallometry has potential implications on the reproductive value of spawning stock biomass, depending on the size composition (demography) of the spawning stock biomass. The present analysis only consider the effects of fish size on egg numbers, and not egg size or quality, which have also been shown to increase with fish size and age (Berkeley et al. 2004, Hixon et al., 2014, Jeuthe et al. 2013, Barneche et al. 2018). Therefore, we might expect an even greater value of the larger older females in the spawning biomass to stock reproductive value.

To illustrate potential implications of size dependent egg production, we used decadal length frequencies of spawning biomass from annual NEFSC spring bottom trawl surveys for each stock, scaled them equally to the same overall biomass, and calculated fecundity. The CC/GOM stock showed a significant decrease in the reproductive value of spawning stock based on length frequencies after the 1990s, and in recent decades productivity declined by more than 15% compared to the 1970s (Figure 3). The GB and SNE stocks did not exhibit strong size truncation in the length frequencies over the period analyzed, and reproductive value was similar across decades (Figures 4 and 5). It is important to note that this calculation assumes the fecundity at

length relation has not changed over time, and that the length frequencies used from the survey are representative of the respective populations. Also, using the length frequencies from the 1970s as the ‘base’ to compare to may be inappropriate, as these stocks have been fished prior to then and may have already experienced significant size truncation. These stocks may be capable of greater reproductive potential than reported here, when the size distributions contain larger individuals.

To further explore remaining variation in fecundity that was not explained by fish size, we explored including relative condition, hepatosomatic index, mean oocyte diameter, stock, year and the interaction of stock and year in GLM framework. The resulting best model (determined by AIC) included all variables and explained 86.7% of the deviance in the data (Table 3). The SNE stock had higher fecundity at length (Figure 6), as was reported in McElroy et al. (2015). Relative condition and hepatosomatic index also had positive effects on fecundity, indicated that heavier fish at length and fish with larger livers had higher fecundity. The fish liver plays a critical role (as the site of vitellogenesis synthesis) in the provision of vitellogenin (yolk) to the developing oocytes. There was a negative relation between the mean oocyte diameter of the developing clutch and fecundity, indicating down-regulation of fecundity during the development process. This has been previously reported, and detailed via quantification of atresia in yellowtail flounder (McElroy et al. 2015). We included mean oocyte diameter as a covariate in fecundity models to account for variation in fecundity related to sampling an individual earlier or later in the development process.

The model indicated significant stock, year, and interaction of stock and year effects (Table 3, Figure 7). While there was coherence across stocks in most years indicating potentially similar environmental forcing of fecundity over a broad geographic scale, in other years fecundity was more variable across stocks suggesting more regional forcing of fecundity. In general, CC/GOM and SNE stock showed slight decline in fecundity, especially between 2014 and 2018, followed by a rebound in 2019 for the SNE stock. The more limited data for the GB stock limits the ability to detect trends over time.

Relative condition as a proxy for fecundity. Given that  $K_n$  was a significant predictor of fecundity, we compared the  $K_n$  of the fecundity fish (confirmed pre spawn developing females) with the macroscopic developing females collected at sea with individual weights. Given that yellowtail flounder are batch spawners, the macroscopic class ‘developing’ contains some individuals that have already released a batch or more of eggs, which affects their total weight and estimated relative condition. We were interested if the patterns in  $K_n$  determined from the fecundity fish with detailed other measures (liver weight, mean oocyte diameter) and confirmed pre spawning status (i.e. no post ovulatory follicles present in histology) were comparable to the patterns in  $K_n$  obtained from developing females collected at sea. Given the later provides a longer time series, strong relations may provide a means to infer prior unmeasured fecundity. For the 10 year time period compared, the annual variation in the two estimates of  $K_n$  tracked reasonably well for each stock. However, given that variation in spawning condition over the entire time series was greater than the variation in the 10 year period of overlap with fecundity (spawning seasonality WP), it is not appropriate to infer trends in  $K_n$  early in the time series are

indicative of fecundity. Using the time series of Kn data from the NEFSC spring bottom trawl surveys to predict fecundity will require disentangling of spawning phenology and physiological condition at the individual level, which may or may not be possible.

### Conclusions

Fecundity scaling is hyper-allometric; a given biomass of large females will produce more eggs than an equal biomass of smaller females.

Given the hyper-allometric fecundity relationship, changes in stock demographics will result in changes in stock reproductive value (notwithstanding abundance). The illustration using spring survey length-frequencies for each stock suggest such changes have occurred in the GOM stock where size truncation has depleted the value of remaining spawning stock. Such truncation was not evident in the GB and SNE stock over the time series evaluated, but they may have already been truncated.

In addition to fish size, relative condition, hepatosomatic index, and mean oocyte diameter explained variation in annual fecundity which varied by stock and year. Variation in fecundity was synchronized across stocks in some years, but not others, suggesting different scales of environmental forcing.

Relative condition has a positive effect on fecundity, suggesting it may be a useful proxy to infer fecundity over a longer time series. However, relative condition is influenced by spawning condition which varies over the time series, complicating its interpretation as an indicator of reproductive potential.

### Literature cited

Barneche, D. R., D. R. Robertson, C. R. White, and D. J. Marshall. 2018. Fish reproductive-energy output increases disproportionately with body size. *Science* 360(6389):642-644.

Berkeley, S. A., C. Chapman, and S. M. Sogard. 2004. Maternal age as a determinant of larval growth and survival in a marine fish, *Sebastes melanops*. *Ecology* 85:1258-1264.

Hixon, M. A., D. W. Johnson, and S. M. Sogard. 2014. BOFFFFs: on the importance of conserving old-growth age structure in fishery populations. *Ices Journal of Marine Science* 71(8):2171-2185.

Jeuthe, H., E. Brannas, and J. Nilsson. 2013. Effects of egg size, maternal age and temperature on egg, viability of farmed Arctic charr. *Aquaculture* 408:70-77.

McBride, R. S., S. Somarakis, G. R. Fitzhugh, A. Albert, N. A. Yaragina, M. J. Wuenschel, A. Alonso-Fernandez and G. Basilone 2015. Energy acquisition and allocation to egg production in relation to fish reproductive strategies. *Fish and Fisheries* 16(1): 23-57.

McElroy, W. D., M. J. Wuenschel, E. K. Towle, and R. S. McBride. 2016. Spatial and annual variation in fecundity and oocyte atresia of yellowtail flounder, *Limanda ferruginea*, in US waters. *Journal of Sea Research* 107:76-89.

Schmidt, T. C. D., J. A. Devine, A. Slotte, M. Claireaux, A. Johannessen, K. Enberg, G. J. Oskarsson, J. Kennedy, Y. Kurita, and O. S. Kjesbu. 2020. Environmental stressors may cause unpredicted, notably lagged life-history responses in adults of the planktivorous Atlantic herring. *Progress in Oceanography* 181.

Schmidt, T. C. D., A. Slotte, J. Kennedy, S. Sundby, A. Johannessen, G. J. Oskarsson, Y. Kurita, N. C. Stenseth, and O. S. Kjesbu. 2017. Oogenesis and reproductive investment of Atlantic herring are functions of not only present but long-ago environmental influences as well. *Proceedings of the National Academy of Sciences of the United States of America* 114(10):2634-2639.

Thorsen, A., and O. S. Kjesbu. 2001. A rapid method for estimation of oocyte size and potential fecundity in Atlantic cod using a computer -aided particle analysis system. *Journal of Sea Research* 46:295-308.

Tomkiewicz, J., M. J. Morgan, J. Burnett, and F. Saborido-Rey. 2003. Available information for estimating reproductive potential of Northwest Atlantic groundfish stocks. *Journal of Northwest Atlantic Fisheries Science* 33:1-21.

Wuenschel, M. J., W. D. McElroy, K. Oliveira, and R. S. McBride. 2019. Measuring fish condition: an evaluation of new and old metrics for three species with contrasting life histories. *Canadian Journal of Fisheries and Aquatic Sciences* 76(6):886-903.

Table 1. Summary of yellowtail flounder fecundity samples analyzed by year, stock area, and source. CP, Cooperative Research gear survey; MADMF, Massachusetts Division of Marine Fisheries inshore trawl survey; SF, NEFSC CRP Study Fleet; HB, NEFSC Bottom trawl Survey.

	<b>GB</b>	<b>GOM</b>	<b>SNE</b>	<b>Grand Total</b>
<b>2010</b>	<b>15</b>	<b>60</b>	<b>60</b>	<b>135</b>
CP	8	18	17	43
MADMF		6		6
SF	7	36	43	86
<b>2011</b>	<b>21</b>	<b>70</b>	<b>48</b>	<b>139</b>
MADMF		15		15
SF	21	55	48	124
<b>2012</b>	<b>17</b>	<b>87</b>	<b>39</b>	<b>143</b>
HB	12	2	5	19
MADMF		1		1
SF	5	84	34	123
<b>2013</b>	<b>54</b>	<b>87</b>	<b>11</b>	<b>152</b>
SF	54	87	11	152
<b>2014</b>	<b>86</b>	<b>55</b>	<b>59</b>	<b>200</b>
HB	32	13	10	55
SF	54	42	49	145
<b>2015</b>	<b>61</b>	<b>113</b>	<b>81</b>	<b>255</b>
HB	16	29	11	56
SF	45	84	70	199
<b>2016</b>	<b>45</b>	<b>125</b>	<b>37</b>	<b>207</b>
HB	23	29	5	57
SF	22	96	32	150
<b>2017</b>	<b>22</b>	<b>117</b>	<b>40</b>	<b>179</b>
HB	22	30	2	54
SF		87	38	125
<b>2018</b>	<b>1</b>	<b>123</b>	<b>56</b>	<b>180</b>
HB	1	22	1	24
SF		101	55	156
<b>2019</b>	<b>13</b>	<b>104</b>	<b>16</b>	<b>133</b>
HB	13	14	1	28
SF		90	15	105
<b>Grand Total</b>	<b>335</b>	<b>941</b>	<b>447</b>	<b>1723</b>

Table 2. Model summary for test of hyperallometry in fecundity vs. weight. Log (Fecundity) ~ Log (Weight).

	<b>Parameter (SE)</b>
Intercept	5.93 (0.125) ***
Log(Weight)	<b>1.33</b> (0.020) ***
Slope test (=1)	p<2e-16 ***
Adj. R-squared	0.713
<i>n fish</i> <i>Oocytes measured</i>	<b>1,722</b> 764,015

Table 3. Summary of significant terms in the fecundity model for yellowtail flounder: Log (Fecundity) ~ Log (TL) + Kn + HSI + MEANOD + Stock + Year + Stock:Year.

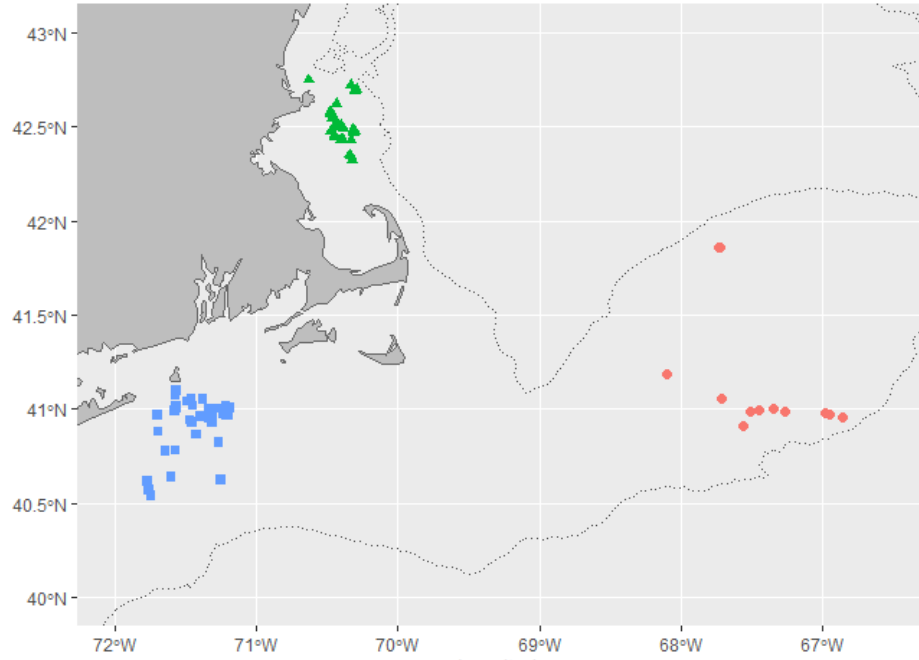
	<b>Significance</b>
Total Length	***
Kn	***
HSI	***
Mean Oocyte Diameter	***
Stock	***
Year	***
Stock:Year	***
Deviance explained (%)	86.7 %
<i>n</i>	1,401



Table 4. NEFSC bottom trawl survey strata used for each Yellowtail Flounder stock unit.

Stock unit	Spring Strata	Fall Strata
GB	Offshore 13-21	Offshore 13-21
CC-GOM	Offshore 25,26,27,39,40, Inshore 56,57,59,60,61,62,64,65,66	Offshore 25,26, 39,40, Inshore 56,57,59,60,61,62,64,65,66
SNE	Offshore 1,2,5,6,9,10,69,73,74 Inshore	Offshore 1,2,5,6,9,10

A)



B)

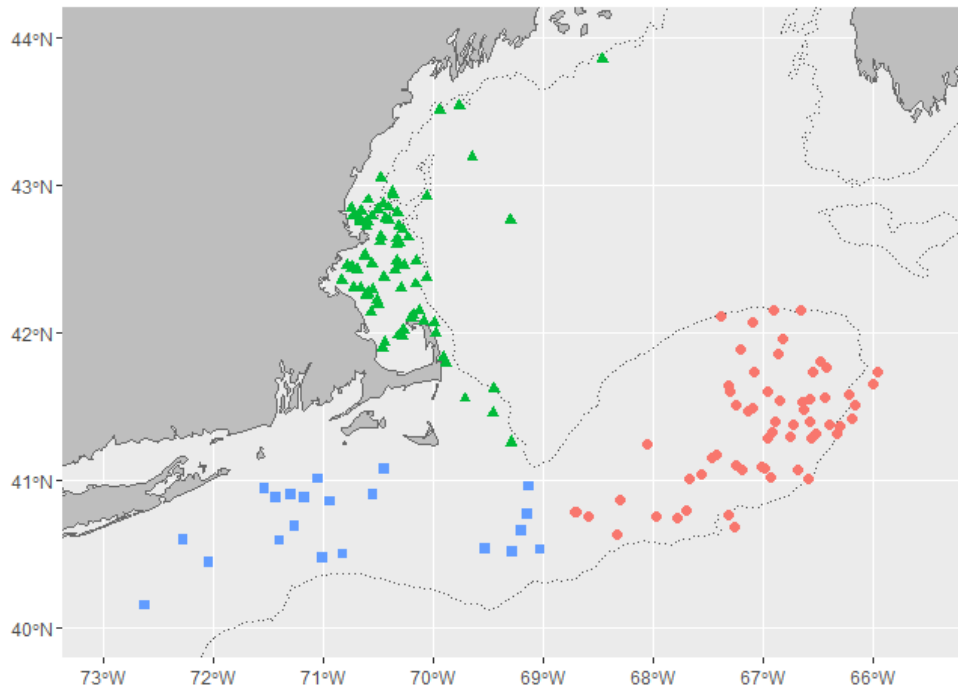


Figure 1. Locations of Yellowtail Flounder sampled from NEFSC Study Fleet (A) and during the NEFSC and MADMF bottom trawl surveys (B). The CC/GOM stock is shown in green, Georges Bank stock shown in red, and Southern New England stock shown in blue.

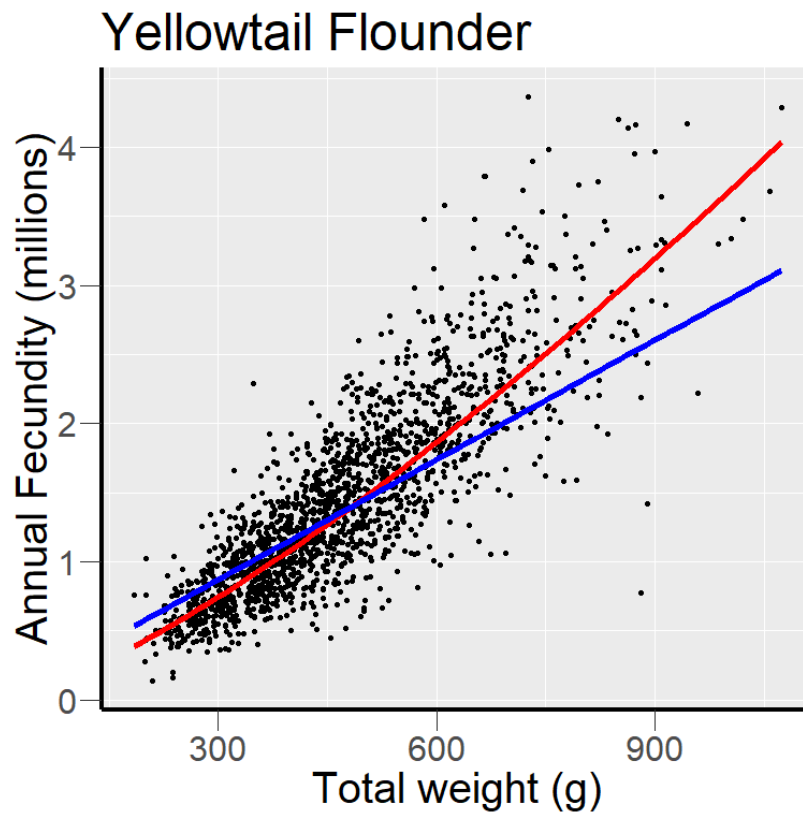


Figure 2. Annual fecundity in relation to body weight of Yellowtail Flounder. The red line is the best fit model with an exponent of 1.33 indicating hyper-allometry. The model fit assuming an isometric relation (fecundity proportional to weight) is shown in blue.

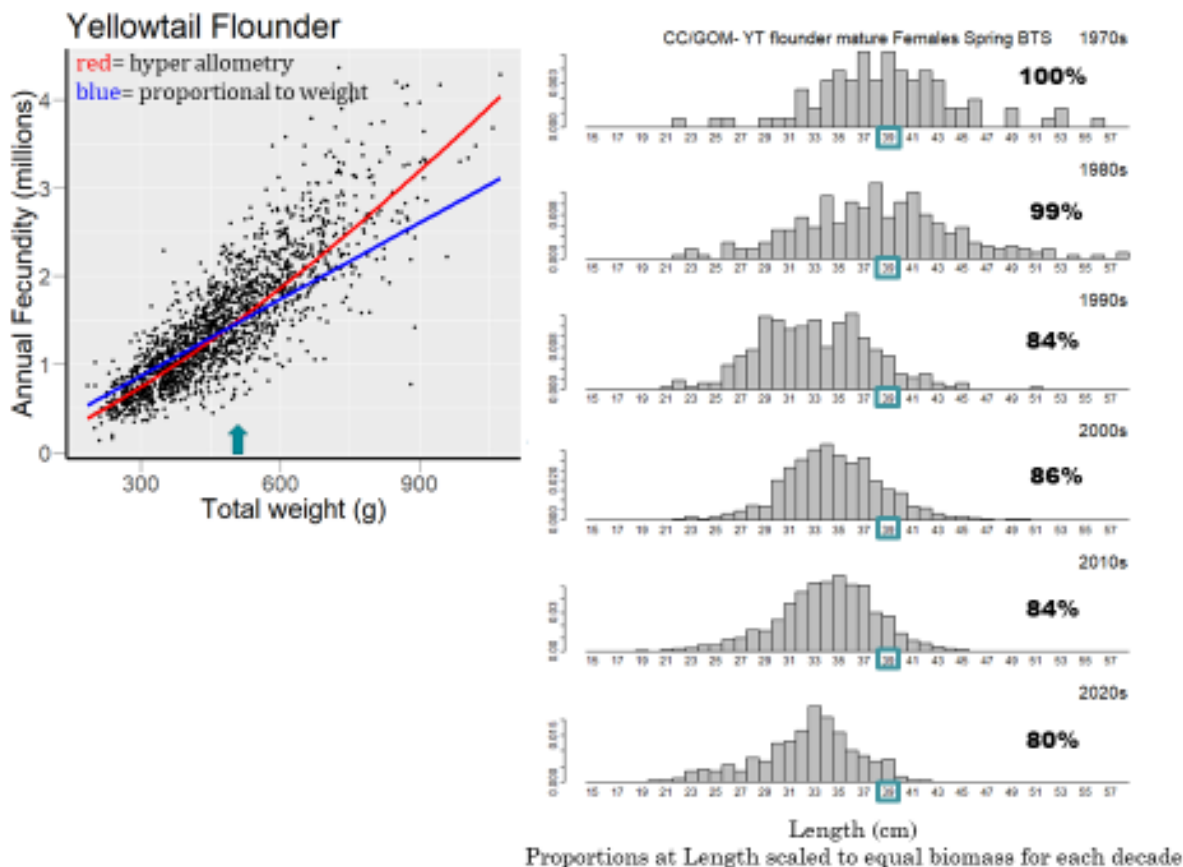


Figure 3. Illustration of the implication of hyperallometric fecundity on CC GOM Yellowtail Flounder. The fecundity relation is shown on the left. On the right are length frequencies of mature females sampled by the NEFSC spring bottom trawl surveys aggregated by decade and scaled to equal biomass using the 1970s as the base. The arrow on left represents approximate weight of 39 cm fish (boxed on right). The percentages shown indicate total fecundity of biomass with that distribution, relative to the base (1970s).

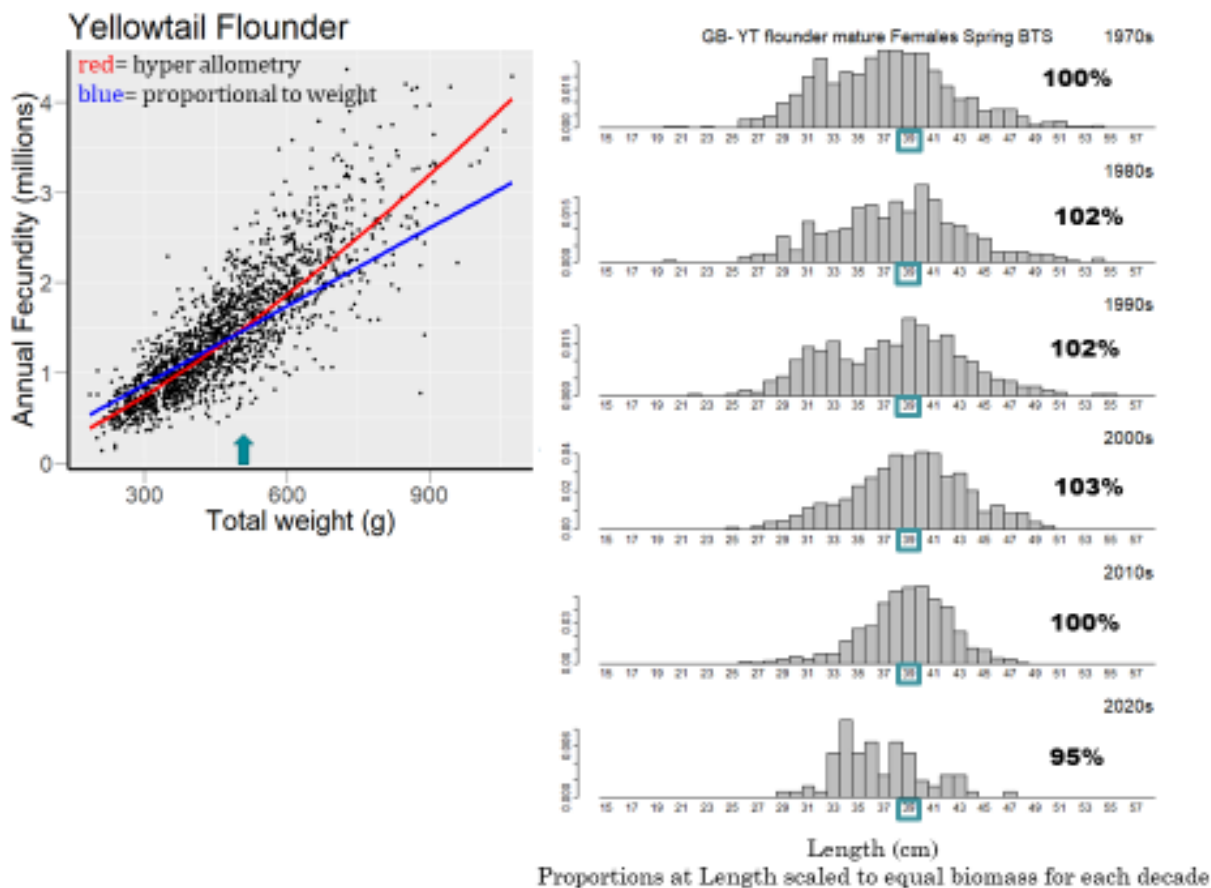


Figure 4. Illustration of the implication of hyperallometric fecundity on GB Yellowtail Flounder. The fecundity relation is shown on the left. On the right are length frequencies of mature females sampled by the NEFSC spring bottom trawl surveys aggregated by decade and scaled to equal biomass using the 1970s as the base. The arrow on left represents approximate weight of 39 cm fish (boxed on right). The percentages shown indicate total fecundity of biomass with that distribution, relative to the base (1970s).

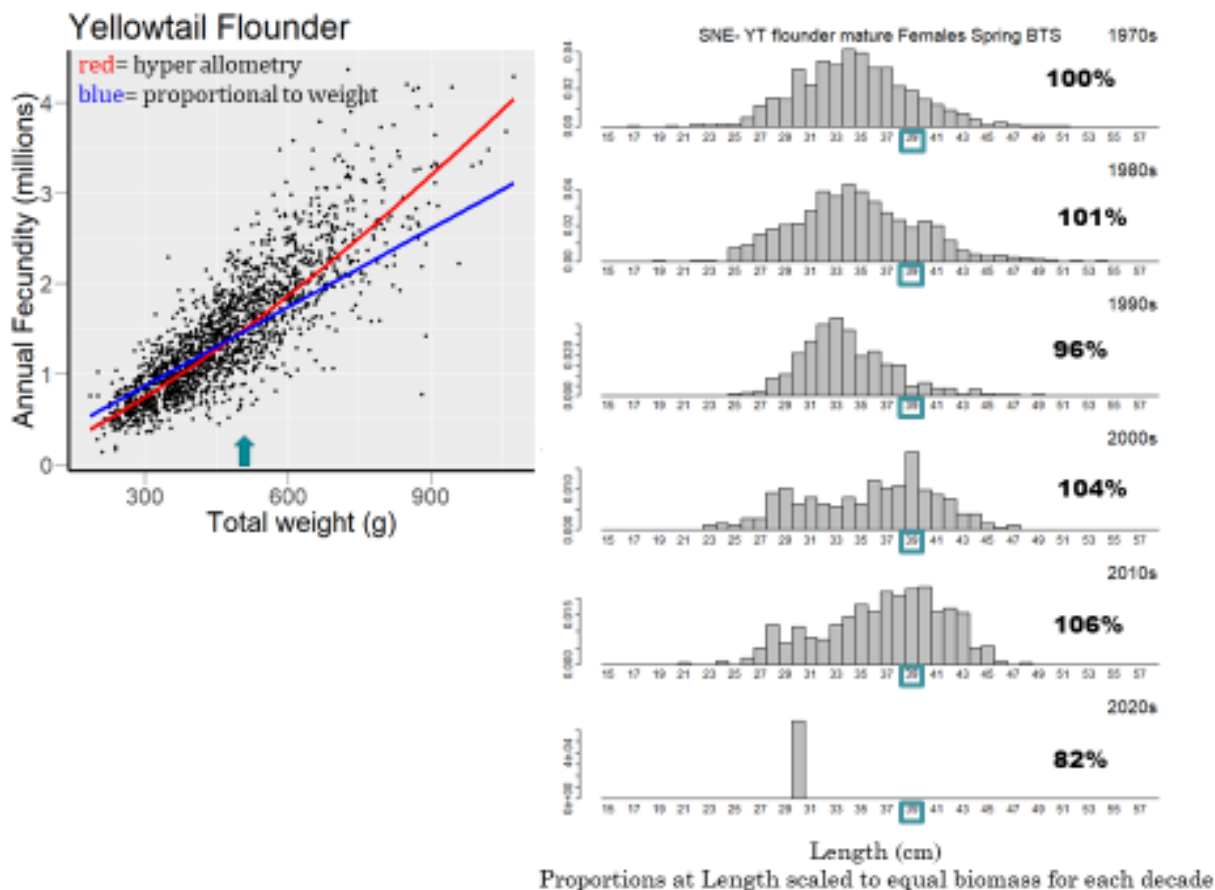


Figure 5. Illustration of the implication of hyperallometric fecundity on SNE Yellowtail Flounder. The fecundity relation is shown on the left. On the right are length frequencies of mature females sampled by the NEFSC spring bottom trawl surveys aggregated by decade and scaled to equal biomass using the 1970s as the base. The arrow on left represents approximate weight of 39 cm fish (boxed on right). The percentages shown indicate total fecundity of biomass with that distribution, relative to the base (1970s).

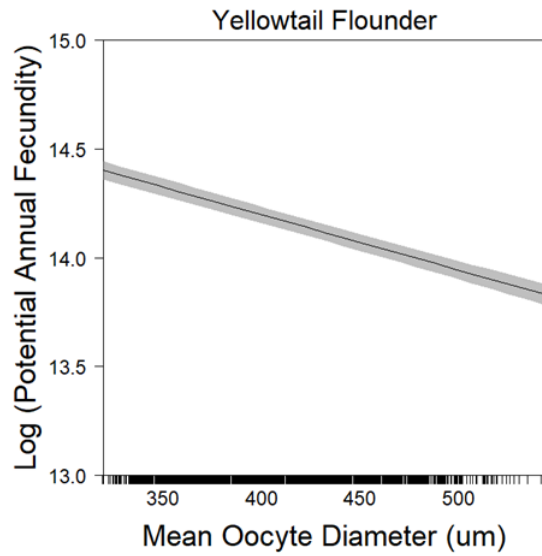
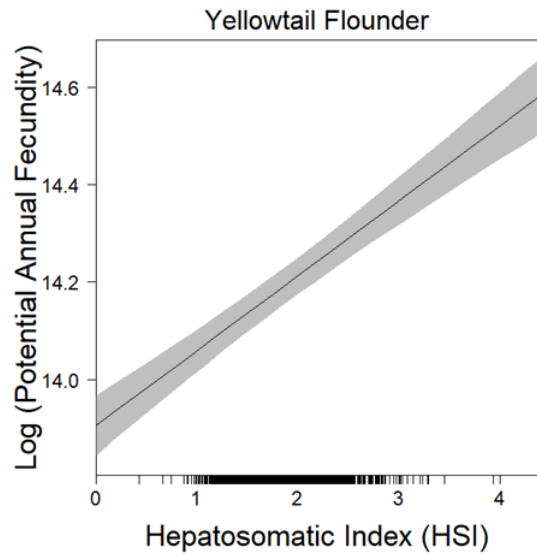
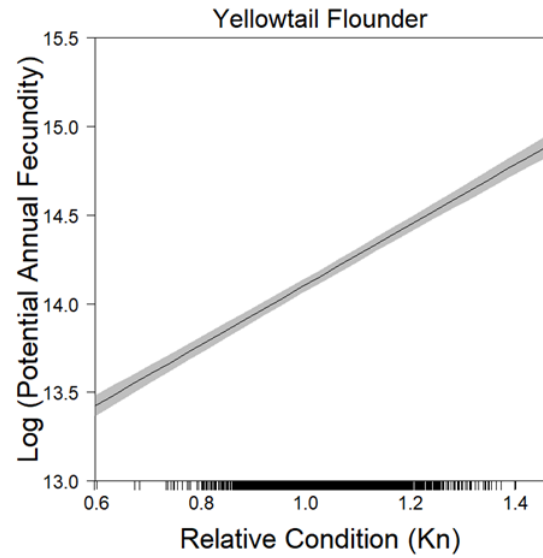
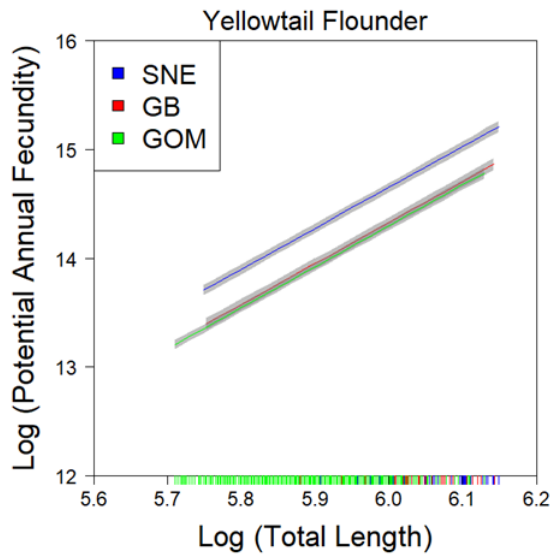
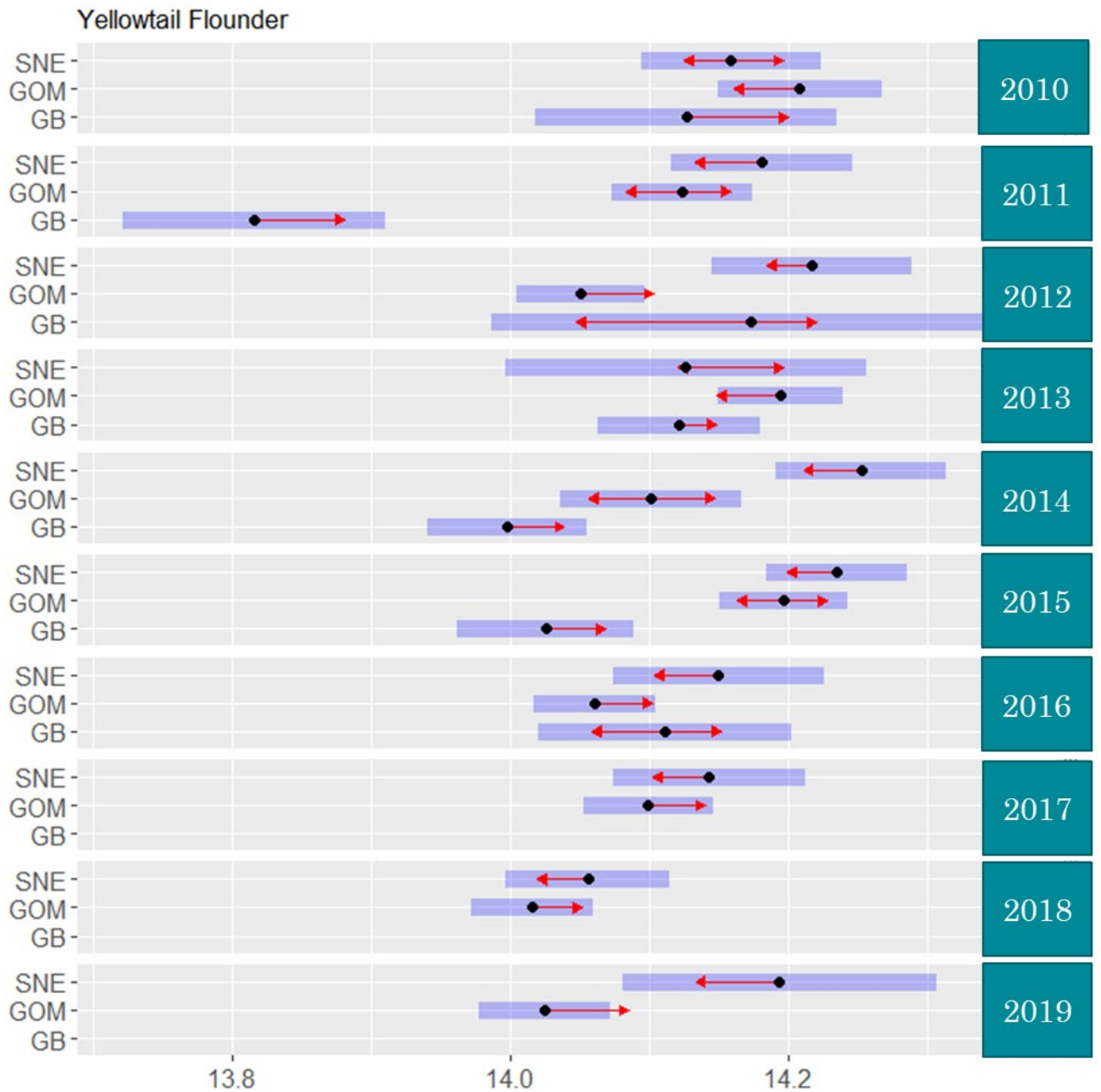


Figure 6. Marginal means partial effects plots for each of the significant quantitative variables in the Yellowtail Flounder fecundity model.



Log (Potential Annual Fecundity)

Figure 7. Marginal means partial effects plots for stock effects by year from the Yellowtail Flounder fecundity model.



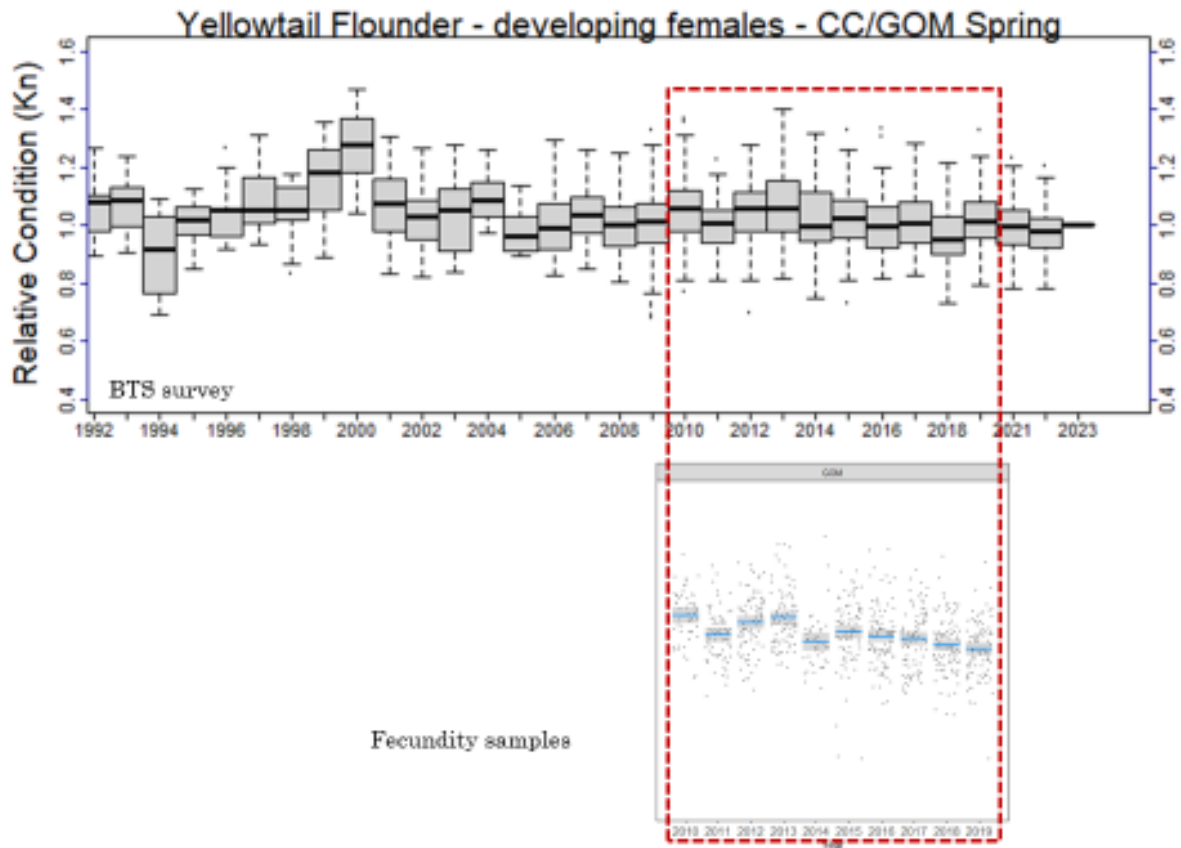


Figure 8. Comparison of trends in relative condition (Kn) for CC/GOM yellowtail flounder mature females collected on the NEFSC spring bottom trawl 1992-2023 to the Kn of fecundity fish analyzed 2010-2019 modeled as a function of hepatosomatic index and mean oocyte diameter.

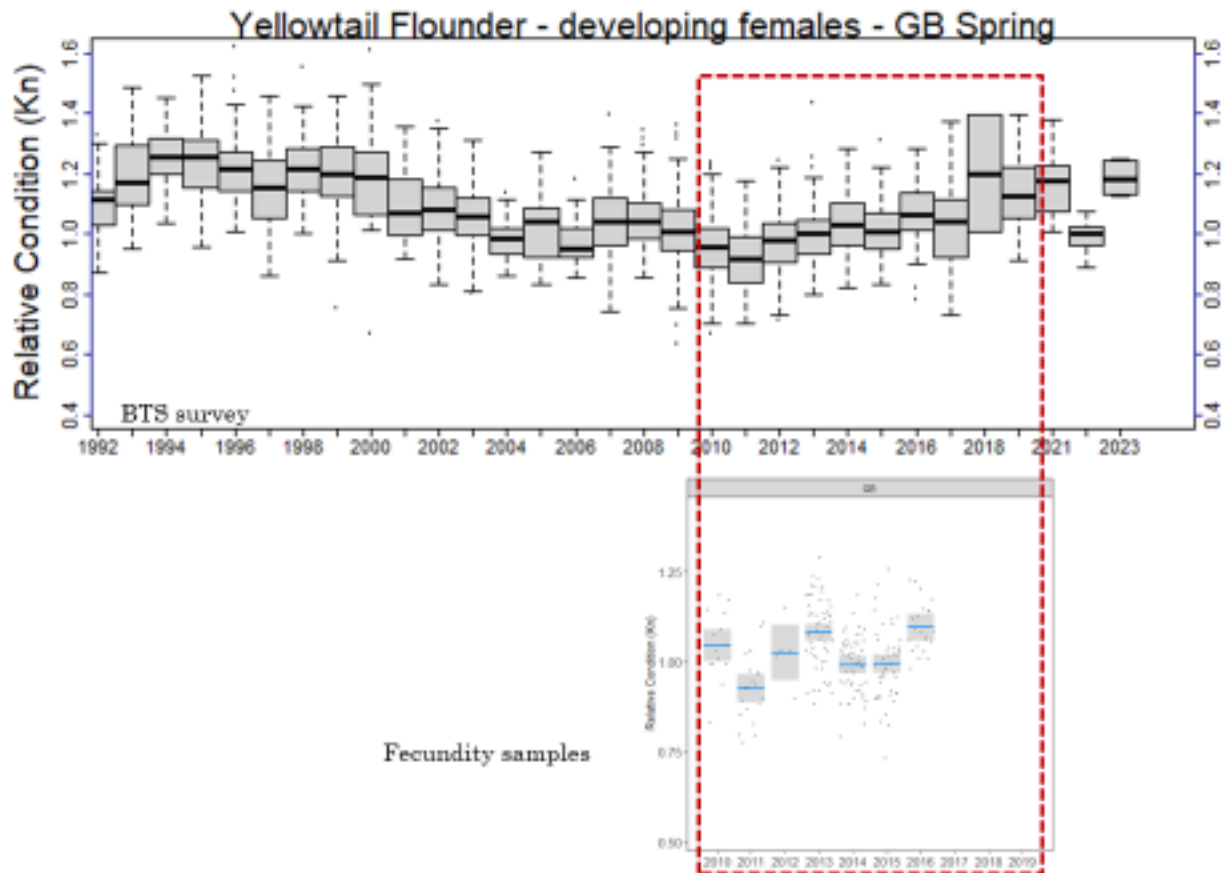


Figure 9. Comparison of trends in relative condition (Kn) for GB yellowtail flounder mature females collected on the NEFSC spring bottom trawl 1992-2023 to the Kn of fecundity fish analyzed 2010-2019 modeled as a function of hepatosomatic index and mean oocyte diameter.

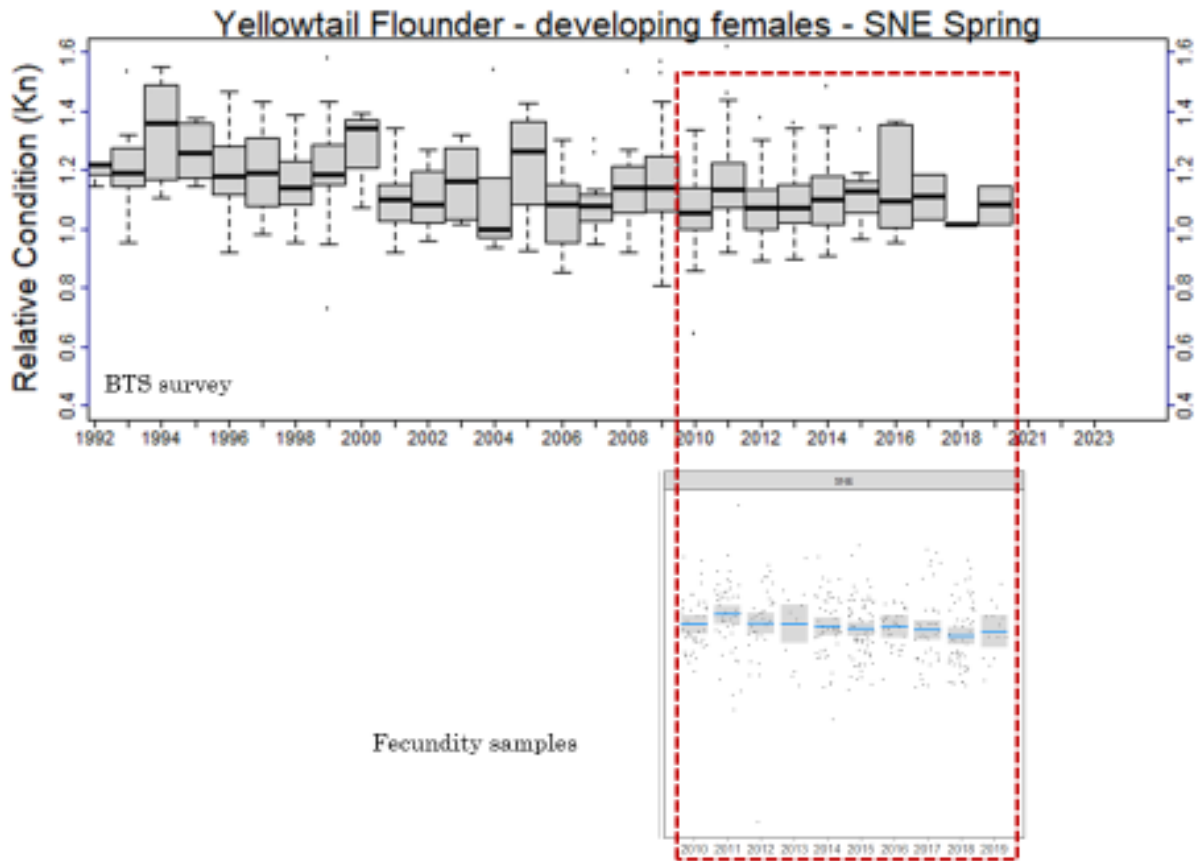


Figure 10. Comparison of trends in relative condition (Kn) for SNE yellowtail flounder mature females collected on the NEFSC spring bottom trawl 1992-2023 to the Kn of fecundity fish analyzed 2010-2019 modeled as a function of hepatosomatic index and mean oocyte diameter.